Journal of Nuclear and Radiochemical Sciences, Vol. 6, No.1, pp. 55-60, 2005

Ion Transport Across a Bilayer Lipid Membrane in the Presence of a Hydrophobic Ion or an Ionophore

Osamu Shirai,*[,a] Akihiro Uehara,[a] Hajimu Yamana,[a] Toshihiko Ohnuki,[b] Yumi Yoshida,[c] and Sorin Kihara[c]

[a]*Research Reactor Institute, Kyoto University, Kumatori, Osaka 590-0494, Japan*
[b]*Advanced Science Research Center, Japan Atomic Energy Research Institute, Tokai, Ibaraki 319-1195, Japan*
[c]*Department of Chemistry, Kyoto Institute of Technology, Matsugasaki, Kyoto 606-8585, Japan*

Received: November 15, 2004; In Final Form: April 21, 2005

The ion transport from one aqueous phase (W1) to another (W2) across a bilayer lipid membrane (BLM) in a cell system in the presence of a hydrophobic ion or an ionophore was investigated by voltammetry. The ion transport current was observed by addition of a small amount of hydrophobic ion such as tetraphenylborate, dipicrylaminate, etc. into W1 or/and W2 containing a hydrophilic salt serving as a supporting electrolyte. The hydrophobic ion was distributed into the BLM with the counter ion to hold the electroneutrality within the BLM. It was pointed out that the counter ion could transfer between W1 and W2 across the BLM since concentrations of the counter ion in W1, BLM, and W2 were so high as to cause the ion transfer current while concentrations of the hydrophobic ion were very low. The facilitated transports of alkali ions across a BLM containing valinomycin (Val) used as an ionophore were also investigated by considering the hydrophobicity of both the objective cation and the counter anion and the formation of the alkali metal ion-Val complex.

1. Introduction

The ion transfer from one aqueous solution (W1) to another (W2) across a bilayer lipid membrane (BLM) has been investigated extensively for a fundamental understanding of the features of ion transfer across biomembranes.[1, 2] An ion transfer current is observed when ion transporters such as ion channel forming peptides and ion carrier compounds are added into the BLM or hydrophobic ions are added to the aqueous phase in the presence of hydrophilic supporting electrolytes, respectively.[2–6] Most of the authors have assumed that the ion transfer current is caused by the transfer of ions associated with the transporter or that of the hydrophobic ion, since only the associated ions or hydrophobic ions can spontaneously distribute from the aqueous phase to the BLM. However, the electroneutrality within the BLM is not held in this mechanism.

We observed that the magnitude of the ion transfer current was proportional, not only to the hydrophobicity of an additive hydrophobic ion but also to that of a counter ion in aqueous phases.[7-9] Then, we discovered that the counter ion spontaneously moved into the BLM with the additive hydrophobic ion and that the counter ion but not the hydrophobic ion transferred across the BLM. On the other hand, it has been recognized that the ion transfer facilitated by an ionophore is attributed to transfer of the ion associated with the ionophore.[2, 10] However, Wittenkeller et al. showed that the ion pair of a cation associated with valinomycin (Val) and a counter anion was distributed between the aqueous phase and the BLM.[11, 12] We found the same distribution of the cation-Val complex and a counter anion as that found by Wittenkeller et al. and observed the continuous transfer of the cation and the anion across the BLM containing Val.[13]

In the present work, ion transfers across a BLM in the presence of hydrophobic ions and facilitated transfers of alkali ions across a BLM containing Val as an ionophore were reviewed from the viewpoint of the distribution of ion pairs between the aqueous phase and the BLM.

*Corresponding author. E-mail: shirai@HL.rri.kyoto-u. FAX: +81-724-51-2634.

2. Experimental

Chemicals. Lipids used to form the BLM were L-α-phosphatidylcholine (Merck, No. 544274), PC, and cholesterol (Wako Pure Chemical Ind., Ltd., No. 087-21), Ch. Valinomycin was purchased from the Sigma Chemical Co. (No. 41K4005).

All other reagents were of reagent grade and used without further purification.

Preparation of BLMs. Two aqueous compartments filled with 15 mL of aqueous solution were separated by a 0.2 mm thick tetrafluoroethylene resin sheet (a product of Mitsui Fluorochemical Co.) as shown in Figure 1. The BLM was obtained as a black lipid membrane by brushing the *n*-decane

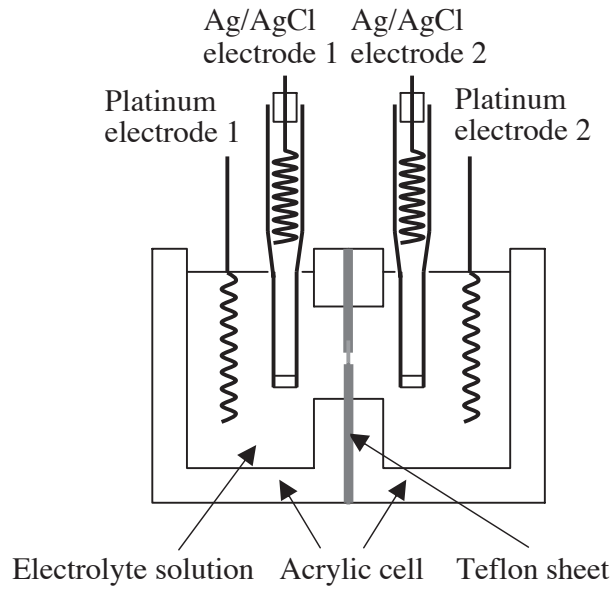

Figure 1. The schematic diagram of the electrochemical cell used in the present study.

Published on Web 07/31/2005

solution of each lipid or both lipids and Val on a 1 mm diameter aperture made in the tetrafluoroethylene resin sheet.[8, 9] The formation of a BLM was confirmed by microscopic observation and capacitance measurement. Valinomycin was dissolved in ethanol at a concentration of 10^{-3} M. Here, M denotes mol dm^{-3}. An adequate volume of ethanol solution was added into a 1 mL flask. After the ethanol was evaporated, the BLM-forming solution was prepared by adding a mixture of Val, ~ 10 mg of PC and ~ 5 mg of Ch with *n*-decane to the flask.

Voltammetric measurement. The BLM system employed in the present study is indicated by eq 1.

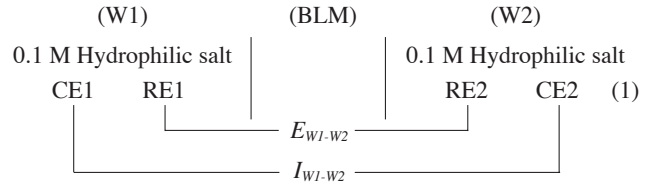

where a hydrophilic salt such as LiCl, NaCl, KCl, RbCl, CsCl, LiBr, NaBr, KBr, RbBr, CsBr, Li_2SO_4, Na_2SO_4, K_2SO_4, Rb_2SO_4, or Cs_2SO_4 was used as the supporting electrolyte in the aqueous phases.

The electrochemical cell used for the voltammetric measurement with a BLM system was essentially the same as that proposed by Tien,[14] and placed in a Faraday cage during the measurement in order to decrease the background noise. The voltammogram for the ion transfer from W1 to W2 across the BLM was recorded by scanning the potential difference between W1 and W2, $E_{W1\text{-}W2}$, and by measuring the current between W1 and W2, $I_{W1\text{-}W2}$. Two silver-silver chloride electrodes, RE1 and RE2, and two platinum wire electrodes, CE1 and CE2, were used to apply the $E_{W1\text{-}W2}$ and to measure $I_{W1\text{-}W2}$, respectively.

All voltammograms were measured by scanning $E_{W1\text{-}W2}$ at a rate of 0.01–0.10 Vs^{-1} at 25 ± 0.5 °C, unless otherwise mentioned.

Apparatus. The potentiostat, the function generator and the X-Y recorder used for the voltammetric measurement were a Model HA-1010mM1A (Hokuto Denko Co.), Model HB-105 (Hokuto Denko Co.) and Model F-5C (Riken Denshi Co.), respectively.

3. Ion Transport Across a BLM by Addition of Hydrophobic Ions into W1 and/or W2 in the Presence of Hydrophilic Electrolytes in W1 and W2

As an example, curve 1 in Figure 2 shows the voltammogram recorded with W1 and W2 containing 0.1 M $MgSO_4$ by scanning $E_{W1\text{-}W2}$ in the region between +0.1 and –0.1 V and, simultaneously, by measuring $I_{W1\text{-}W2}$. No current peak was observed in the voltammogram. Similar voltammograms were observed when KCl, NaCl, $MgCl_2$, K_2SO_4, and Na_2SO_4 were used as hydrophilic salts in W1 and W2 instead of $MgSO_4$.[8, 9]

By the addition of one of extremely hydrophobic ions of either dipicrylaminate, DPA^-, or tetraphenylborate, $TPhB^-$, into W1 of the cell system (1) (Curves 2 and 3 in Figure 2), a pair of well established positive and negative peaks symmetrical about the origin (the point of 0 V and 0 A) appeared, even though the concentration of the added hydrophobic ion was very dilute, less than 10^{-6} M.[7–9] The half-peak potentials of both the positive and negative peaks were determined to be around 0 V.

When DPA^- was added into W1, the peak current density was nearly proportional to the concentration of DPA^- in the range between 5×10^{-8} and 10^{-5} M and to the square root of the scan rate of $E_{W1\text{-}W2}$ in the range between 0.01 and 0.1 Vs^{-1}. As shown in Table 1, the current density increased slightly with the increase of the concentration of the hydrophilic salt,

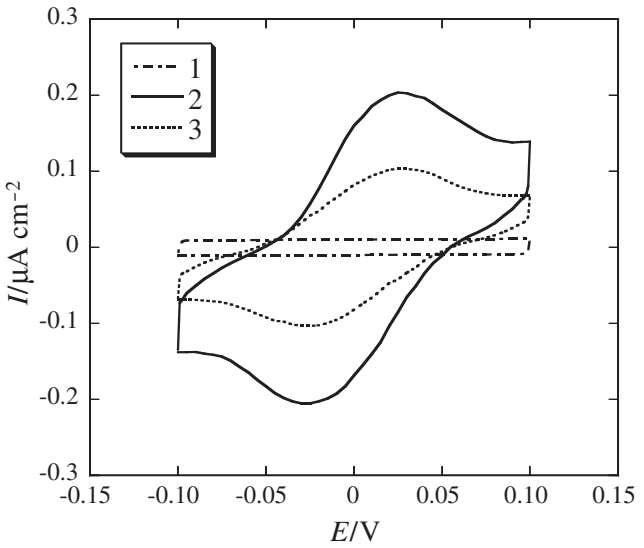

Figure 2. Voltammograms for the ion transfer through a BLM composed of PC and Ch. Curve 1: 0.1 M $MgSO_4$ in both W1 and W2. Curves 2 and 3: same as curve 1, but in the presence of 10^{-6} M DPA^- in W1 (curve 2) and 10^{-6} M $TPhB^-$ in W1 (curve 3). Scan rate of $E_{W1\text{-}W2}$: 0.01 Vs^{-1}.

TABLE 1: Peak Current Densities in Cyclic Voltammograms Observed with the Addition of DPA^-, $TPhB^-$, and CV^+ to be 10^{-6} M[9]

Supporting electrolyte in W1 and W2	Peak current density / μA cm^{-2} Ion added in W1 (10^{-6} M)		
	DPA^-	$TPhB^-$	CV^+
0.1 M $MgSO_4$	0.20 ± 0.03	0.10 ± 0.02	0.04 ± 0.01
1 M $MgSO_4$	0.23 ± 0.03	0.12 ± 0.02	0.05 ± 0.01
0.1 M K_2SO_4	0.60 ± 0.10	0.25 ± 0.03	0.04 ± 0.01
0.1 M Na_2SO_4	0.22 ± 0.03	0.12 ± 0.02	0.04 ± 0.01
0.1 M $MgBr_2$	0.21 ± 0.03	0.12 ± 0.02	0.05 ± 0.01
0.1 M $MgCl_2$	0.20 ± 0.03	0.11 ± 0.02	ca. 0
0.2 M KCl	0.62 ± 0.10	0.23 ± 0.03	ca. 0
0.2 M NaCl	0.19 ± 0.03	0.13 ± 0.02	ca. 0

$MgSO_4$, in aqueous phases from 0.1 to 1 M, and increased when the hydrophilic salt in aqueous phases was changed from 0.1 M $MgSO_4$ to 0.1 M K_2SO_4 or 0.1 M Na_2SO_4. By adding the same amount of $TPhB^-$ instead of DPA^- into W1 of the system in the presence of 0.1 M $MgSO_4$ in W1 and W2, the characteristics of the voltammogram were similar to those with DPA^-, except that the peak current density was smaller. Similar voltammograms were also observed by the addition of dilute (5×10^{-7} to 10^{-5} M) crystalviolet, CV^+, or ethylviolet, EV^+, into one of two aqueous phases containing 0.1 M $MgSO_4$ or $MgBr_2$, respectively. The peak current densities depended on the species of the anion in the hydrophilic salt, but were practically independent from the hydrophilic cation in the salt, as shown in Table 2.[9, 15] Here, standard Gibbs free energy can be regarded as the measure of the hydrophobicity of the ion. It is well known in liquid-liquid extraction chemistry that the distribution coefficient of the ion pair depends on hydrophobicities of the added ion and the counter ion. Similarly, the hydration energy can be also regarded as the measure of the hydrophobicity (Table 3).

These results introduced a new ion transfer mechanism shown in Figure 3. Not only the hydrophobic ion (A^- or C^+) but also the counter ion (i^+ or j^-) are distributed from the aqueous phase to the BLM. In the case of the addition of hydrophobic ions such as DPA^-, $TPhB^-$, CV^+, and EV^+, the added ion and the counter ion are distributed to be about 10^{-4} M. Therefore, the ion transfer current in the voltammogram is

TABLE 2: Standard Gibbs Free Energies for Transfers, ΔG_{tr}^{0}, of Various Ions from Aqueous, W, to nitrobenzene, NB,[8] 1,2-dichloroethane, DCE,[8] or Acetonitrile, AN[15]

Ion	W/NB ΔG_{tr}^{0}/kJ mol^{-1}	W/DCE ΔG_{tr}^{0}/kJ mol^{-1}	W/AN ΔG_{tr}^{0}/kJ mol^{-1}
DPA^-	−39.4		
$TPhB^-$	−35.9	−35.1	−32.4
Pic^-	−4.6		−4
ClO_4^-	8.0	17.2	2
Br^-	28.4	38.5	31.3
Cl^-	31.4	46.4	42.1
SO_4^{2-}	>67.3		
EV^+	ca.-44*		
CV^+	−39.5		
$TPhAs^+$	−35.9	−35.1	−32.8
$TPenA^+$	−35.1	−34.7	
TBA^+	−24.0	−21.8	−31
$TPrA^+$	−10.0	−8.8	−13
TEA^+	−5.7	4.2	−7
TMA^+	3.4	17.6	3
K^+	23.4		8.1
Na^+	34.2		15.1
Mg^{2+}	69.6		

TABLE 3: The Molar Gibbs Free Energies of the Hydration of Ions[18]

Cation	ΔG_{tr}^{0}/kJ mol^{-1}	Anion	ΔG_{tr}^{0}/kJ mol^{-1}
Li^+	475	F^-	465
Na^+	365	Cl^-	340
K^+	295	Br^-	315
Rb^+	275	I^-	275
Cs^+	250	ClO_4^-	205
$TPhAs^+$	−50	$TPhB^-$	−50

attributable to the transfer of the counter ion, since the concentration of the hydrophobic ion in W1 and W2 is negligible and the counter ion exists sufficiently in W1, BLM, and W2. When the hydrophobic ion was added into both aqueous phases, the peak height became larger than that observed when the hydrophobic ion was added only in W1 (e.g. about 1.6 times when 10^{-6} M DPA^- was added in the aqueous phases containing 0.1 M $MgSO_4$).

In the voltammograms that were obtained by the addition of one of the hydrophobic cations such as tetrapentylammonium, $TPenA^+$, tetrabutylammonium, TBA^+, and tetraphenylarsonium, $TPhAs^+$, at concentrations of 10^{-5} to 10^{-4} M into W1 of the cell system, a pair of positive and negative currents of different magnitudes appeared around the origin. Curve 1 in Figure 4 is the voltammogram that was recorded by adding 10^{-4} M $TPenA^+$ into W1 and 0.1 M $MgSO_4$ into both W1 and W2. When one of the hydrophobic cations was added into both W1 and W2 phases, positive and negative peaks symmetrical about the origin appeared in the voltammogram (curve 2 in Figure 4). The magnitudes of the positive and negative peaks (or limiting currents) were proportional to the concentration of the hydrophobic cation added in the range between 10^{-5} and 10^{-4} M, while the ratio of the positive to negative peak (or limiting current) was almost constant. The ratio depended on the kind of hydrophobic cation that was added. Since the hydrophobicities of these ions are generally smaller than those of DPA^-, $TPhB^-$, CV^+, and EV^+ as shown in Table 2, the distribution ratios of an ion pair of the added hydrophobic ion and the counter ion between the aqueous phase and the BLM phase

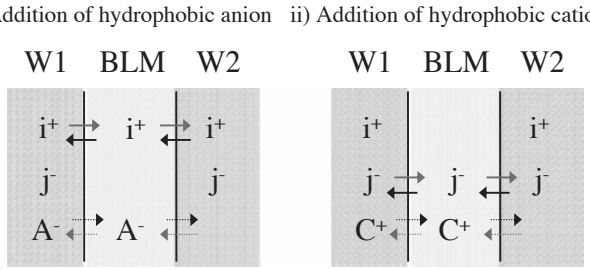

Figure 3. Ion transfer mechanisms with the addition of a hydrophobic anion and hydrophobic cation. i^+: hydrophilic cation, j^-: hydrophilic anion, A^-: hydrophobic anion and C^+: hydrophobic cation.

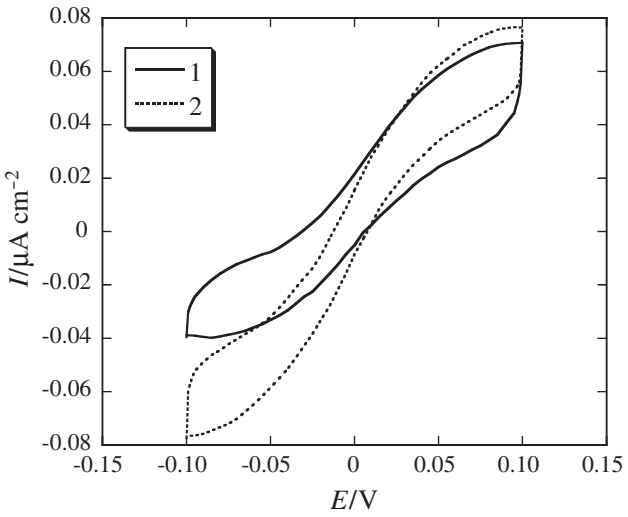

Figure 4. Voltammograms for ion transfer through a BLM composed of PC and Ch. Curve 1: 10^{-4} M $TPenA^+$ in W1 and 0.1 M $MgSO_4$ in both W1 and W2. Curve 2: same as curve 1, but in the presence of 10^{-4} M $TPenA^+$ in W1 and W2.

were smaller than those for the ions having higher hydrophobicity. As the distribution ratio was smaller, the concentration of the additive hydrophobic ion needs to be higher to maintain a constant ion transfer current. When the concentration of the additive hydrophobic ion in aqueous phase was higher than ~ 10^{-4} M, a difference in magnitude between the cathodic and anodic current peaks was observed in the voltammogram (Figure 4). The anodic current is caused by the transfer of the counter ion while the cathodic current is attributed to both the transfer of the added hydrophobic ion and that of the counter ion. These results indicate that the transfer of the added hydrophobic ion from the aqueous phase to the BLM cannot be ignored at concentrations of the hydrophobic ion higher than 10^{-4} M.

When the hydrophobicity of the added ion is weaker than those of the above-mentioned ions, the hydrophobic ion should be added to reach a concentration greater than 10^{-4} M in the aqueous phase. Curve 1 in Figure 5 is a typical result when 10^{-3} M of picrate, Pic-, was added in W1 in the presence of 0.1 M $MgSO_4$ in W1 and W2. Current densities at $E_{W1\text{-}W2} = -0.1$ (the final descent) and +0.1 V (the limiting current) depended on the concentrations of both Pic^- and Mg^{2+} in W1. When 10^{-3} M Pic^- was added into both aqueous phases, a symmetry of the final rise and the final descent about the origin was observed, as seen as curve 2 of Figure 5.

When a hydrophobic ion was added into one of two aqueous phases in the presence of a hydrophilic salt, the voltammogram was transformed depending on the properties and concentration of the added hydrophobic ion. It can be assumed that the distribution equilibrium of the ion pair between W and BLM is similar to that between W and organic phase; Org. Equation 2 holds between the distribution ratios, D_M and D_X, of a cation, M^+, and an anion, X^-, and the standard Gibbs transfer free

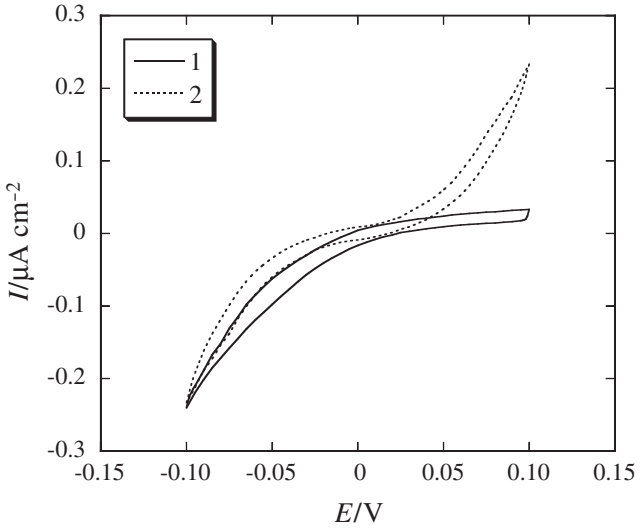

Figure 5. Voltammograms for the ion transfer through a BLM composed of PC and Ch. Curve 1: 10^{-3} M Pic^- in W1 and 0.1 M $MgSO_4$ in both W1 and W2. Curve 2: same as curve 1, but in the presence of 10^{-3} M Pic^- in W1 and W2.

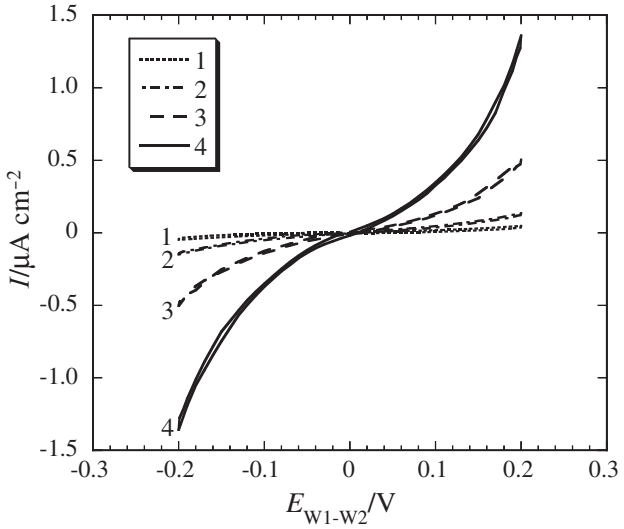

Figure 6. Cyclic voltammograms for ion transfer across a BLM containing Val between W1 and W2 in the presence of 0.1 M KCl. Potential scanning rate: 0.01 Vs^{-1}. Temperature: 298 ± 1 K. Concentration of Val in the BLM-forming *n*-decane solution: 10^{-6} (curve 1); 3×10^{-6} (curve 2); 10^{-5} (curve 3); 3×10^{-5} M (curve 4).

energies of M^+ and X^- from W to Org, $\Delta G_{tr,M}{}^0$ and $\Delta G_{tr,X}{}^0$, when W containing a salt, $M^+ \cdot X^-$, is equilibrated with an equivolume of Org.[16]

$$\ln D_M = \ln D_X = 1/2 \{-(\Delta G_{tr,M}{}^0 + \Delta G_{tr,X}{}^0)/RT \qquad (2)$$

Similarly, the distribution ratios of an ion pair of the added hydrophobic ion and the counter ion between aqueous and BLM phases can be represented. Accordingly, the waveform of the observed voltammogram and the magnitude of ion transfer current depended on both the hydrophobicity and concentration of the added hydrophobic and counter ions. When a hydrophobic ion such as DPA^-, $TPhB^-$, CV^+, or EV^+ is added into W1 and/or W2, the additive hydrophobic ion behaves as a carrier of the counter ion within the BLM.

Here, the hydration energy is used as the index of the hydrophobicity. Taking into account the hydration energies of various ions (Table 3) and the transfer energies of various ions from aqueous to Org (Table 2), Cs^+ and I^- can transfer more easily than K^+ and Cl^-, respectively. Bender and Tien reported that waveforms of voltammograms obtained by the addition of I^- and I_3^- were the same as those obtained by the addition of Pic^- and DPA^-, respectively.[17] When CsCl was used as a hydrophilic electrolyte instead of KCl, the background current in the case of CsCl was larger than that in the case of KCl. This would be one of reasons that ^{137}Cs and ^{129}I, which are generated by nuclear fission of ^{235}U, accumulate in living organisms more easily than other alkali metal ions and halogen ions, respectively.

4. Ion Transport across a BLM Containing Val as an Ionophore

It has been proposed that an ionophore such as Val or dibenzo-18-crown-6 serves as a carrier compound for complex-forming ions.[2, 10] However, the role of the ionophore in the ion transfer is still under debate. By considering the electroneutrality within the BLM and the ion transport mechanism described in the previous section, the role of the ionophore in the ion transport across the BLM containing Val as an ionophore has been studied.

Figure 6 shows cyclic voltammograms for the ion transfer between W1 and W2 containing 0.1 M KCl across a BLM of PC and Ch containing Val. When Val was added to a BLM formed from the *n*-decane solution containing 10^{-6} to 3×10^{-5} M Val, the cyclic voltammograms were symmetrical about the

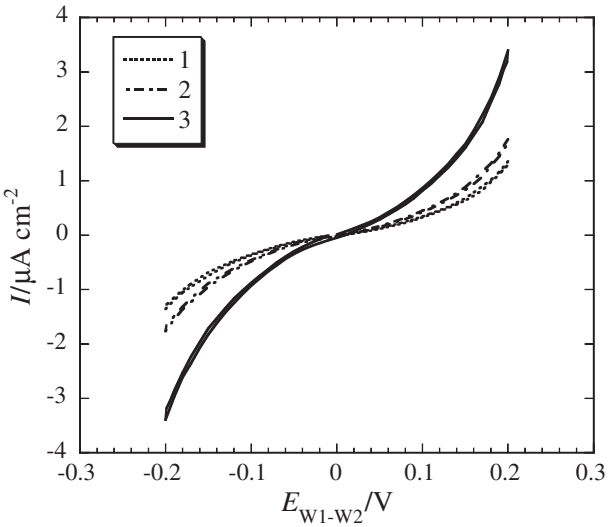

Figure 7. Cyclic voltammograms for the ion transfer across a BLM containing Val. Potential scanning rate: 0.01 Vs^{-1}. Temperature: 298 ± 1 K. Concentration of Val in the BLM-forming *n*-decane solution: 3×10^{-5} M. Electrolyte in W1 and W2: 0.1 M KCl (curve 1); 0.1 M KBr (curve 2); 0.1 M $KClO_4$ (curve 3).

origin, (0 V, 0 A). In the absence of Val in the BLM, no ion transfer current was observed in the voltammogram by scanning $E_{W1\text{-}W2}$ between –0.1 and 0.1 V and measuring $I_{W1\text{-}W2}$. The absolute value of $I_{W1\text{-}W2}$, $|I_{W1\text{-}W2}|$, increased with an increase in $|E_{W1\text{-}W2}|$. The current density at a specific $E_{W1\text{-}W2}$ was reproducible to about ± 10% on each run. The ion transfer current at a specific $E_{W1\text{-}W2}$ was not dependent on the scan rate of $E_{W1\text{-}W2}$ in the region from 0.01 to 0.50 Vs^{-1}. This means that the ion permeation across the BLM is the rate-determining step. The magnitude of $I_{W1\text{-}W2}$ would be attributed to the electric resistance of the BLM. As shown in Figure 6, the magnitude of $I_{W1\text{-}W2}$ at a specific $E_{W1\text{-}W2}$ was proportional to the concentration of Val in the BLM-forming *n*-decane solution in the range from 10^{-6} to 3×10^{-5} M. The molar ratios of PC : Ch : Val in the *n*-decane solutions containing 10^{-6}, 3×10^{-6}, 10^{-5}, and 3×10^{-5} M Val were, then, assumed to be about $1 : 1 : 10^{-3}$, $1 : 1 : 3 \times 10^{-3}$, $1 : 1 : 10^{-2}$, and $1 : 1 : 3 \times 10^{-2}$, respectively. Therefore, the magnitude of $I_{W1\text{-}W2}$ at a specific $E_{W1\text{-}W2}$ was also proportional to the molar ratios of PC : Ch : Val.

Figure 7 shows the cyclic voltammograms for the ion transfer across a BLM containing Val between W1 and W2

containing 0.1 M KCl, KBr and $KClO_4$. These waveforms were also analogous to that in Figure 6. The magnitude of $I_{W1\text{-}W2}$ at a definite $E_{W1\text{-}W2}$ was altered by a change in anion species. The magnitude of $I_{W1\text{-}W2}$ at 0.1 V increased with the increasing ionic radii of the anionic species. This disagrees with the current magnitudes estimated by the conventional concept that only K^+ can transfer across a BLM. In all cases, the magnitude of the ion transfer current at a definite $E_{W1\text{-}W2}$ is directly proportional to the concentration of Val in the BLM. The transfers of alkali metal ions from W1 and W2 to the BLM are facilitated by the formation of a complex with Val in the BLM by analogy with studies on facilitated ion transfer at the interface between aqueous and organic solutions.[16, 17] If only the alkali ion is distributed from W1 or W2 to the BLM, the electroneutrality is not maintained within the BLM phase. The authors suggested that the complex-forming ion was distributed with the counter ion from W1 and/or W2 to the BLM in the presence of Val in the BLM.[13] Wittenkeller et al. pointed out that the alkali metal ion was distributed from W1 and W2 to the BLM containing Val with the counter anion as an ion pair.[11, 12] It can be assumed that the distribution equilibrium of the ion pair between W and BLM is similar to that between W and Org phases as written in eq 2. In this case, the stabilization of the cation by complex formation with Val should be estimated. The distribution ratio, D_M, of a cation, M^+, is denoted using the standard Gibbs transfer free energies of M^+ from W to Org, $\Delta G_{tr,M}{}^0$, and the effect of activity change of the cation in Org, $\ln (1 + K_{st} C_{ligand})$, when W containing a salt, $M^+ X^-$, is equilibrated with an equivolume of Org.[16] Therefore, eq 2 can be rewritten as follows:

$$\begin{aligned} \ln D_M &= \ln D_X \\ &= 1/2 \{-(\Delta G_{tr,M}{}^0 + \Delta G_{tr,X}{}^0)/RT + \ln (1 + K_{st} C_{ligand})\} \\ &= -(\Delta G_{tr,M}{}^* + \Delta G_{tr,X}{}^0)/2RT, \end{aligned} \quad (3)$$

where, C_{ligand} indicates the concentration of the ligand in Org, and K_{st} is the stability constant of the M^+-ligand complex in Org. $\Delta G_{tr,M}{}^*$ is then the seeming transfer energy of M^+ from W to Org, and $\Delta G_{tr,M}{}^*$ is defined by the relation $\Delta G_{tr,M}{}^* = \Delta G_{tr,M}{}^0 - \ln (1 + K_{st} C_{ligand})$. Equation 3 does not involve the formation of ion pairs in either W or Org phases, and the activity coefficients of M^+ and X^- in W and Org phases are regarded as unity. This indicates that *DM* depends not only on $\Delta G_{tr,M}{}^0$ but also on $\Delta G_{tr,X}{}^0$ and the stabilization achieved by forming the complex. Similarly, pairs of K^+ and the counter ion will be distributed from the aqueous phase to the BLM. Therefore, it is thought that the currents flowing at both the W1|BLM and BLM|W2 interfaces are caused by the transferring of not only K^+ but also the counter ions, ClO_4^-, Br^-, and Cl^-. Since the ion permeability depends on the ion concentration, the diffusion coefficients in the aqueous and BLM phases, the ion absorption, the ion pair formation, and the complex formation, it is thought that the magnitude of the current of the anion transfer is not always equal to that of the cation transfer. Figure 8 shows the relation between the hydration energy of the anions in Table 3[18] and the logarithmic magnitude of the ion transfer current at 0.1 V in Figure 7. Here, the hydration energies of ClO_4^-, Br^-, and Cl^- are used instead of the transfer energies from the aqueous phase to the BLM, since the transfer energies from the aqueous phase to the BLM cannot be evaluated. It is suggested that the logarithmic magnitude of the ion transfer current depends on the hydrophobicity of the counter anion.

The ion transfer mechanism, shown in Figure 9, is actually somewhat more complex. Based on previous findings on the voltammetry of the ion transfer across the interface between two immiscible electrolyte solutions, a simplified version of the ion transfer mechanism can be described as follows: At the initial condition, the concentration of the ion pair of an alkali metal ion with a counter anion in the BLM is negligibly low.

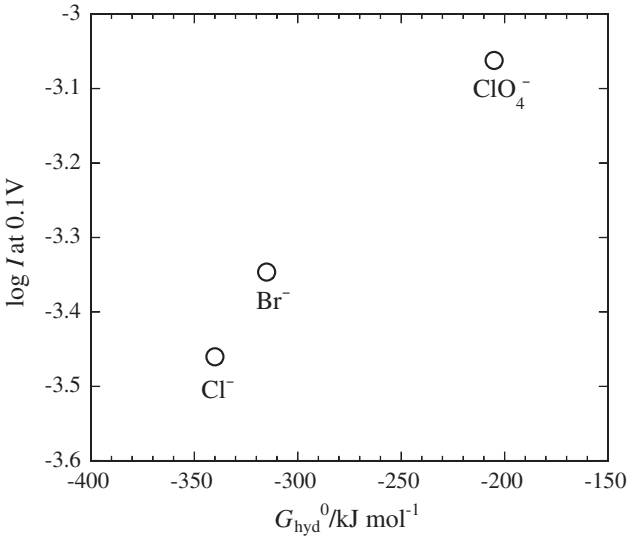

Figure 8. The relationship of log *I* to hydration energy of anion.

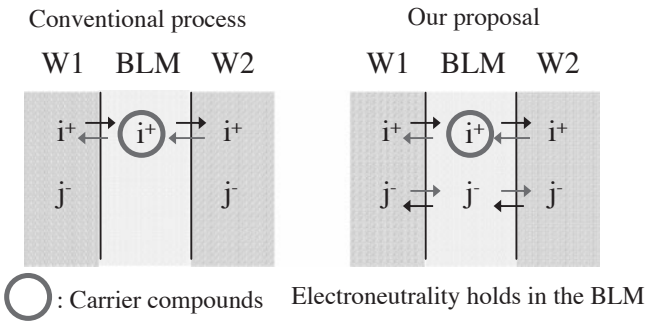

Figure 9. The ion transfer mechanism of the ion transfer across the BLM.

In the presence of Val in the BLM, the alkali metal ion spontaneously penetrates into the BLM with the counter anion. By applying the $E_{W1\text{-}W2}$, the alkali metal ion in the W1 phase then transfers to the W2 phase across the BLM, and the counter anion transfers in the opposite direction from W2 to W1 phases at the same time. Sato et al. suggested that the anion transport occurred independently from the cation transport.[10] If their suggestion is correct, the ion transfer current of the counter anion should be observed in the absence of Val in the BLM. However, there is no distinct current wave in the voltammogram in the absence of Val. Accordingly, the anion transport probably depends on the cation transport.

The cyclic voltammograms for ion transfer across a BLM containing Val with 0.1 M LiCl, NaCl, RbCl, or CsCl are shown in Figure 10. The magnitude of $I_{W1\text{-}W2}$ at a definite $E_{W1\text{-}W2}$ was altered by a change in the cation species. When LiCl, NaCl, KCl, RbCl, or CsCl was used as the supporting electrolyte, the magnitude of $I_{W1\text{-}W2}$ at 0.1 V was 8.7, 13, 350, 1400, or 2100 nA cm^{-2}, respectively. The magnitude of $I_{W1\text{-}W2}$ at a definite $E_{W1\text{-}W2}$ was also proportional to the concentration of Val in the BLM.

There are many research reports on the conductivities of BLMs containing both alkali metal ions in the aqueous phases and Val.[6, 19, 20] Although several authors reported that the conductivity of a BLM using RbCl as an electrolyte was greater than that using CsCl, the orders of the conductivities in most of the results were almost consistent with that of the present result. It is usually thought that only an alkali metal ion complexing with Val is distributed from W1 and/or W2 to the BLM, and the ion transfer current is attributed to the transfer of the alkali metal ion across the BLM between W1 and W2. The magnitude of the ion transfer current was then postulated to depend on the stability constants for the complex formation, since the alkali metal ions could not transfer across

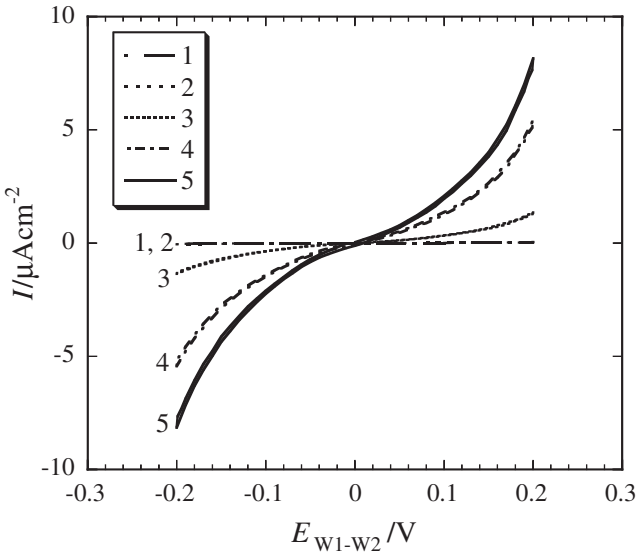

Figure 10. Cyclic voltammograms for the ion transfer across a BLM containing Val. Potential scanning rate: 0.01 Vs^{-1}. Temperature: 298 ± 1 K. Concentration of Val in the BLM-forming *n*-decane solution: 3 × 10^{-5} M. Electrolyte in W1 and W2: 0.1 M LiCl (curve 1); 0.1 M NaCl (curve 2); 0.1 M KCl (curve 3); 0.1 M RbCl (curve 4); 0.1 M CsCl (curve 5).

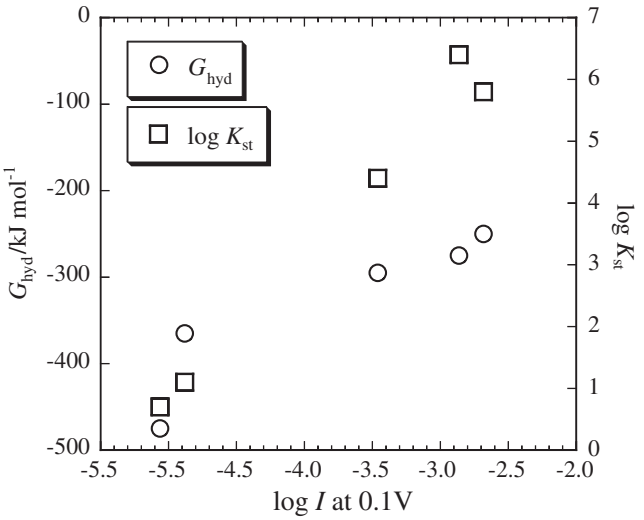

Figure 11. The dependence of log *I* on the hydration energy of cation and on the stability constant of the Val-cation complex.

the BLM in the absence of Val in the BLM.

According to our result on anion transport and findings on the voltammetry for facilitated ion transfer between W and Org, the ion transfer energy from W to BLM results from the sum of its own transfer energy and the stability of the cation in the BLM by complex formation with a ligand as described by eq 3. The third right-hand term of eq 3 represents the potential shift caused by the stabilization of M^+ with the ligand in the BLM. At the same C_{ligand}, the concentration of M^+ in the BLM, depends on both $\Delta G_{\mathrm{tr,\,M}}{}^0$ and K_{st}. Figure 11 shows the relation between the hydration energy of the alkali metal ions and the ion transfer current and that between the stability constant of the alkali metal ion-Val complex in the acetonitrile and the ion transfer current.[21] For the calculation, hydration energies are used instead of transfer energies from the aqueous phase to the BLM, since the transfer energies of the alkali metal ions from the aqueous to the BLM would mainly depends on the hydration energies and the exact values of transfer energies cannot be evaluated. Similarly, the stability constants in acetonitrile are utilized instead of those in the BLM, since the stability constants in the BLM cannot be determined. Based on these results, it is suggested that the magnitude of the ion transfer current depends on both the hydrophobicity of the alkali metal ion and the stabilization by the complex formation.

4. Conclusion

In the present paper, ion transport from one aqueous phase to another across a BLM in the presence of hydrophobic ions or Val was investigated based on the voltammetric concept and method. It was found that not only hydrophobic ions or complex-forming ions with an ionophore but also counter ions were distributed from the aqueous phase to the BLM. By applying an electric potential between two aqueous phases, the alkali metal ion in one aqueous phase (W1) transfers to another aqueous phase (W2) across the BLM and the counter anion transfers in the opposite direction (from W2 to W1) at the same time. These results suggest that an ionophore acts as a carrier of cation transport across the BLM.

Acknowledgment. The authors wish to thank Dr. K. Maeda of the Kyoto Institute of Technology for his useful comments.

References

(1) H. T. Tien, *Bilayer Lipid Membranes*, Marcel Dekker, New York (1974).
(2) R. B. Genis, *Biomembranes*, Springer-Verlag, New York (1989).
(3) J. Koryta, *Ions, Electrodes and Membranes, 2nd ed.* Wiley, Chichester (1991).
(4) D. J. Aidley and P. R. Stanfield, *Ion Channels*, Cambridge University Press, Cambridge (1996).
(5) G. A. Woolley and B. A. Wallace, J. Membrane Biol. **129**, 109 (1992).
(6) R. T. Hamilton and E. W. Kaler, J. Membrane Sci. **54**, 259 (1990).
(7) O. Shirai, S. Kihara, M. Suzuki, K. Ogura, and M. Matsui, Anal. Sci., 7th suppl. 607 (1991).
(8) O. Shirai, S. Kihara, Y. Yoshida, and M. Matsui, J. Electroanal. Chem. **389**, 61 (1995).
(9) O. Shirai, Y. Yoshida, M. Matsui, K. Maeda, and S. Kihara, Bull. Chem. Soc. Jpn. **69**, 3151 (1996).
(10) H. Sato, H. Hakamada, Y. Yamazaki, M. Uto, M. Sugawara, and Y. Umezawa, Biosens. Bioelectron. **13**, 1035 (1998).
(11) L. Wittenkeller, D. M de Freitas, and R. Ramasamy, Biochem. Biophys. Res. Commun. **184**, 915 (1992).
(12) L. Wittenkeller, W. Lin, C. Diven, A. Ciaccia, F. Wang, and D. M de Freitas, Inorg. Chem. **40**, 1654 (2001).
(13) O. Shirai, H. Yamana, T. Ohnuki, Y. Yoshida, and S. Kihara, J. Electroanal. Chem. **570**, 219 (2004).
(14) H. T. Tien, Prog. Surf. Sci. **19**, 169 (1985).
(15) Y. Marcus, Pure Appl. Chem. **55**, 977 (1983).
(16) Y. Yoshida, M. Matsui, O. Shirai, K. Maeda and S. Kihara, Anal. Chim. Acta **373**, 213 (1998).
(17) D. Homolka, L. Q. Hung, A. Hafmanová, M. W. Khalil, J. Koryta, V. Mareček, Z. Samec, S. K. Sen, P. Vanýsek, J. Weber, M. Březina, M. Janda, and I. Stibor, Anal. Chem. **52**, 1606 (1980).
(18) Y. Marcus, J. Chem. Soc. Faraday Trans. **87**, 2995 (1991).
(19) P. Läuger, Science **178**, 24 (1972).
(20) G. Favero, L. Campanella, A. D'Annibale, R. Santucci, and T. Ferri, Microchem. J. **74**, 141 (2003).
(21) A. Hafmanová, J. Koryta, M. Březina, T. H. Ryan, and K. Angelis, Inorg. Chim. Acta **37**, 135 (1979).